

half-occupancy of the band. If we choose the zero-order Hamiltonian to be the Hartree one, for which

$$\mu_0 = \frac{1}{2} I, \quad (D3)$$

while simultaneously removing the Hartree part of the interaction potential, we find no change in chemical potential as the interaction is turned on. On the other hand, there are no anomalous diagrams. All such diagrams would contain interaction lines between like-spin particles which is impossible in the Hubbard Hamiltonian. It is then easy to see that

$$E' = 0, \quad (D4)$$

and under these conditions the Goldstone expansion for the energy is valid. But then the Goldstone energy is independent of any one-body potential that may be added to the unperturbed Hamiltonian and subtracted from the interaction part as long as the Fermi surface remains the same. Since this is the case for the Hartree potential in our analysis, we can safely conclude that the Goldstone expansion using the noninteracting Hamiltonian to zero order is also valid.

*Supported in part by the Office of Naval Research, Contract No. 78721 and by the Canadian National Research Council.

†Permanent address: Department of Physics, University of Sherbrooke, Sherbrooke, Quebec, Canada.

‡Permanent address: Department of Metallurgy, Mechanics and Materials Science and Department of Biophysics, Michigan State University, East Lansing, Mich. 48823.

¹G. Kemeny and L. G. Caron, *Rev. Mod. Phys.* **40**, 790 (1968).

²J. Hubbard, *Proc. Roy. Soc. (London)* **A276**, 238 (1961); **A281**, 401 (1964).

³B. D. Day, *Rev. Mod. Phys.* **39**, 719 (1967).

⁴To first order in the perturbation one need not worry about possible breakdown of the Goldstone expansion due to nonsphericity of the Fermi surface. See W. Kohn and J. M. Luttinger, *Phys. Rev.* **118**, 41 (1960).

⁵For the very special case of the half-filled Hubbard band in the tight-binding limit, it is shown in Appendix D that the Goldstone formalism is exact even though the

Fermi surface is nonspherical.

⁶T. Matsubara and T. Yokota, in *Proceedings of the International Conference on Theoretical Physics, Kyoto and Tokyo*, 1953 (Science Council of Japan, Tokyo, 1954), p. 693.

⁷D. Adler, in *Solid State Physics*, edited by F. Seitz, D. Turnbull, and H. Ehrenreich (Academic, New York, 1968), Vol. 21.

⁸J. Des Cloizeaux, *J. Phys. Radium* **20**, 606 (1959); **20**, 751 (1959).

⁹D. R. Penn, *Phys. Rev.* **142**, 350 (1966).

¹⁰N. F. Mott, *Proc. Phys. Soc. (London)* **62**, 416 (1949); *Can. J. Phys.* **34**, 1356 (1956); *Nuovo Cimento Suppl.* **7**, 312 (1958); *Rev. Mod. Phys.* **40**, 677 (1968).

¹¹J. C. Slater, *Quantum Theory of Molecules and Solids*, (McGraw-Hill, New York, 1963), Vol. I.

¹²G. Kemeny and L. G. Caron, *Phys. Rev.* **159**, 768 (1967).

¹³J. M. Luttinger and J. C. Ward, *Phys. Rev.* **118**, 1417 (1960).

Supercurrent Density Distribution in Josephson Junctions

R. C. Dynes and T. A. Fulton

Bell Telephone Laboratories, Murray Hill, New Jersey 07974

(Received 19 November 1970)

The form of the modulation of the critical dc Josephson current I_c of a tunnel junction by an applied magnetic field B is shown to be uniquely related to the supercurrent density distribution within the junction integrated over the direction of B . This relation is used to quantitatively determine these "current-density profiles" from $I_c(B)$ measured for Sn-oxide-Sn junctions with barriers prepared by plasma-discharge oxidation and for the novel light-sensitive junctions described by Giaever, in which the tunneling barrier is formed by an evaporated film of CdS.

I. INTRODUCTION

In the field of tunneling between metals and semiconductors¹ the production of a uniform tunneling barrier has been a long-standing problem. Such techniques as thermal oxidation,² plasma-discharge oxidation,³ anodization⁴ or evaporation of thin insulating films⁵ all have been employed. Usually at

best only indirect evidence of the barrier perfection has been available.

A direct means of investigating this question is presented by the dc Josephson effect.^{6,7} As Josephson has shown, a supercurrent can flow by the tunneling mechanism for junctions between two superconductors. The maximum supercurrent density that can flow at any point is proportional to the

tunneling probability at that point. For such junctions an applied magnetic field B modulates the magnitude I_c of the critical supercurrent,⁸ as first demonstrated experimentally by Rowell.⁹ In the most familiar example B is applied to a rectangular junction of dimensions a and b , parallel to, say, the b dimension. If the tunneling barrier is uniform and self-field effects are negligible, $I_c(B)$ has a Fraunhofer shape of $|(\sin\frac{1}{2}\beta a)/(\frac{1}{2}\beta a)|$, where β is a normalized measure of B to be defined. In practice the experimental $I_c(B)$ in this geometry always departs from this form, one reason being that the junction tunneling barrier and supercurrent density distribution are not uniform.

In this work we discuss the relation between the shape of the $I_c(B)$ of a rectangular junction and the supercurrent density distribution within the junction, based on a connection between the two by Fourier transformation. In Sec. II we present the formal relationship and describe methods for deriving information in practice about the supercurrent density distribution from the $I_c(B)$. In Sec. III we describe the experimental procedures and pitfalls, and in Sec. IV we analyze experimental $I_c(B)$ curves for Sn-oxide-Sn tunnel junctions with a barrier formed by plasma-discharge oxidation and for the novel Sn-CdS-Sn light-sensitive tunneling junctions first investigated by Giaever.¹⁰

II. THEORY

Consider a rectangular tunnel junction lying in the x - y plane with sides parallel to the x and y axes and extending to $x = \pm\frac{1}{2}a$ and $y = \pm\frac{1}{2}b$. The junction has an average barrier thickness d and supports a tunneling supercurrent density in the z direction of

$$J_z(x, y) = J(x, y) \sin\varphi(x, y),$$

where $J(x, y)$ is the maximum current density at the point (x, y) and $\varphi(x, y)$ is the phase difference at (x, y) between the order parameters of the superconductors on either side of the tunnel junction. The phase differences at the two points (x_1, y_1) and (x_2, y_2) obey the relation

$$\varphi(x_2, y_2) - \varphi(x_1, y_1) = 2\pi\Phi/\Phi_0,$$

where $\Phi_0 = h/2e$ is the flux quantum and Φ is the amount of magnetic flux linking a loop joining the two points and extending well beyond the penetration depth λ into the superconductors on either side. The superconductors we take to be thick on the scale of λ . Suppose that Φ is due to an applied field B in the y direction, so that

$$\varphi(x_2, y_2) - \varphi(x_1, y_1) = 2\pi B(2\lambda + d)(x_2 - x_1)/\Phi_0.$$

Then the total tunneling supercurrent is the integral

$$I(B, \varphi_0) = \int_{-b/2}^{b/2} dy \int_{-a/2}^{a/2} dx J(x, y)$$

$$\times \sin[2\pi B(2\lambda + d)x/\Phi_0 - \varphi_0], \quad (1)$$

where the reference phase φ_0 is $\varphi(0, 0)$, the phase difference at the junction center. The *observed* critical current $I_c(B)$ of the junction for fixed B is just the maximum of $I(B, \varphi_0)$ obtainable by varying φ_0 . If we use the normalized magnetic field unit $\beta = 2\pi(2\lambda + d)B/\Phi_0$ and define $\mathcal{J}(x)$ as

$$\mathcal{J}(x) = \int_{-b/2}^{b/2} J(x, y) dy,$$

then (1) becomes

$$I(B, \varphi_0) = \text{Im}[e^{-i\varphi_0} \int_{-a/2}^{a/2} dx \mathcal{J}(x) e^{i\beta x}]. \quad (2)$$

We denote the complex Fourier transform of $\mathcal{J}(x)$ by

$$\mathcal{G}(\beta) = \int_{-a/2}^{a/2} dx \mathcal{J}(x) e^{i\beta x}. \quad (3)$$

Consequently, the experimental quantity $I_c(\beta)$ is

$$I_c(\beta) = |\mathcal{G}(\beta)|; \quad (4)$$

i. e., $I_c(\beta)$ is the magnitude of the complex Fourier transform of a "current density profile" $J(x)$ which is the current density at the point x integrated over the y direction. It is convenient to extend the limits of the integrals to $\pm\infty$ and take the cutoff at $\pm\frac{1}{2}a$ as part of the shape of $J(x)$.

We can write $\mathcal{G}(\beta)$ as $\mathcal{G}(\beta) = I_c(\beta) e^{i\theta(\beta)}$, where $\theta(\beta)$ is real. To construct $\mathcal{J}(x)$ one must know both $|\mathcal{G}(\beta)| = I_c(\beta)$ and $\theta(\beta)$. To determine $\theta(\beta)$ we use a Hilbert-transform procedure which, in principle, gives an exact recovery of $\theta(\beta)$. As an alternative we also employ an approximate but simple reconstruction of $\mathcal{J}(x)$ based on the assumption that $\mathcal{J}(x)$ is nearly an even function of x .

The Hilbert transform relates $I_c(\beta)$ and $\theta(\beta)$ by the formula¹¹

$$\theta(\beta) = \frac{\beta}{2\pi} \int_{-\infty}^{\infty} db \frac{\ln I_c(b) - \ln I_c(\beta)}{\beta^2 - b^2}. \quad (5)$$

The use of this procedure depends upon the fact that $\mathcal{J}(x)$ (except in isolated instances) has a "minimum-phase property." From $\theta(\beta)$ and $I_c(\beta)$ one can then reconstruct the current density profile

$$\mathcal{J}(x) = (1/2\pi) \int_{-\infty}^{\infty} d\beta I_c(\beta) e^{i[\theta(\beta) - \beta x]}. \quad (6)$$

Actually the \mathcal{J} produced in this transform, if (5) is used to obtain the phase, is shifted such that it extends from 0 to a rather than from $-\frac{1}{2}a$ to $+\frac{1}{2}a$. Such a shift corresponds to the addition of a term $\frac{1}{2}\beta a$ to $\theta(\beta)$. For simplicity we shall refer to the profile as $\mathcal{J}(x)$ regardless of the position of the origin.

The second, simpler approach to construct $\mathcal{J}(x)$

is based on the assumption that $\mathcal{J}(x)$ is an approximately even function. Let $\mathcal{J}_0(x)$ and $\mathcal{J}_e(x)$ be, respectively, the odd and even parts of $\mathcal{J}(x)$, and let

$$C(\beta) = \int_{-\infty}^{\infty} dx \mathcal{J}_e(x) \cos \beta x,$$

$$S(\beta) = \int_{-\infty}^{\infty} dx \mathcal{J}_0(x) \sin \beta x$$

denote the transforms of these two functions. Then $\mathcal{J}(\beta)$ is $\mathcal{J}(\beta) = C(\beta) + iS(\beta)$, and $I_c(\beta)$ is $|\mathcal{J}(\beta)| = [C^2(\beta) + S^2(\beta)]^{1/2}$.

Suppose \mathcal{J}_0 vanishes. Then $\mathcal{J}(\beta)$ is real and $I_c(\beta) = |C(\beta)|$. If $\mathcal{J}(x)$ were constant for $|x| \leq \frac{1}{2}a$, $I_c(\beta)$ would have the $|\sin(\frac{1}{2}\beta a)/(\frac{1}{2}\beta a)|$ form, for which the nodes are evenly spaced and correspond to integral numbers of applied flux quanta being present in the barrier and the penetration depths of the adjacent superconductors. If $\mathcal{J}(x)$ is even but not constant, $C(\beta)$ will in most cases still oscillate between positive and negative values with diminishing amplitude so that $I_c(\beta)$ will vanish at particular values of β , but the nodes will no longer be evenly spaced or correspond exactly to integral numbers of applied flux quanta. This deviation must be taken into account if the spacing between the nodes is used to determine λ .

Now suppose $\mathcal{J}_0(x)$ is not zero. Then $I_c(\beta) = [C^2(\beta) + S^2(\beta)]^{1/2}$ is always nonzero unless by chance $C(\beta)$ and $S(\beta)$ vanish simultaneously. If, however, \mathcal{J}_0 is small compared to \mathcal{J}_e in the sense that $|C(\beta)|^2 \gg |S(\beta)|^2$ for most β , then $I_c(\beta)$ will be approximately equal to $|C(\beta)|$ except near the zeros of $C(\beta)$, where the value of $S(\beta)$ becomes important. In this case to a good approximation the minima $I_c(\beta)$ occur at $|C(\beta)| = 0$, and the magnitude of $I_c(\beta)$ at these minima will give the value of $|S(\beta)|$ at these points. If experimentally $I_c(\beta)$ consists of well-defined maxima separated by deep minima we may assume that $\mathcal{J}(x)$ is approximately even and construct $\mathcal{J}_e(x)$ assuming that $|C(\beta)| \approx I_c(\beta)$, taking alternate lobes of the pattern as positive and negative and interpolating linearly through the minima. The heights of the minima then give a semiquantitative measure of the odd part of $\mathcal{J}(x)$.

III. EXPERIMENT

The junctions are formed between two evaporated rectangular strips of Sn or Pb in the perpendicular crossed-strip geometry, giving a rectangular or square junction of typical dimensions ~ 0.2 mm. The barriers are formed by thermal or plasma-discharge oxidation, or by evaporation of an insulating material such as CdS. The junctions are immersed in liquid He. Stray magnetic fields are excluded by a μ -metal can having an internal field $\lesssim 10^{-2}$ G, and the magnetic field B is applied to the junction by a solenoid whose axis lies parallel

to the junction edges. The critical current I_c is monitored using a Pacific Measurements CRT display converter in conjunction with a Tektronix 561 oscilloscope. The current-voltage characteristic of the junction is displayed on the oscilloscope at a repetition rate of a few hundred Hz, and the converter is adjusted to sample the current magnitude at the voltage onset in each cycle. This current I_c is recorded on one axis of an x - y recorder against B on the other axis, giving a continuous plot of $I_c(B)$ as B is swept. Both positive and negative critical currents, denoted $I_{c+}(B)$ and $I_{c-}(B)$, are recorded for a range of B symmetric about $B=0$.

For these junctions $I_c(B)$ typically approximates the Fraunhofer form. The largest I_c (a few mA or less) occurs at $B \approx 0$, and I_c oscillates with increasing B , approaching zero at roughly evenly spaced minima (~ 1 G spacing) and increasing between to maxima lying on a generally decreasing envelope. Several factors may distort these $I_c(B)$ from the ideal shape of Eq. (4). Among these are stray external B fields, trapped flux in the films, self-field effects, noise, and shorts. These affect the $I_c(B)$ in different characteristic ways, as follow.

The stray magnetic field B_s from sources other than trapped flux is nearly uniform at the junction in our experiments. It may be resolved into components B_{sx} and B_{sy} perpendicular and parallel to the applied B . The B_{sy} causes small obvious shifts in the B scale of $I_c(B)$, while B_{sx} enters the integral (1) so that $I_c(B)$ is actually the magnitude of the Fourier transform of the complex quantity

$$\int_{-b/2}^{b/2} dy J(x, y) \exp[2\pi i(2\lambda + d)B_{sx}y/\Phi_0].$$

For the 10^{-2} G stray fields here, however, this quantity is essentially $\mathcal{J}(x)$.

In the absence of stray magnetic fields the $I_c(B)$ should obey the symmetry requirement

$$I_{c+}(+B) = -I_{c-}(-B). \quad (7)$$

Stray fields associated with trapped flux cause this relation to be violated. In these experiments we found that the $I_c(B)$ usually either obeyed (7) to the precision of the measurement (allowing for a small offset in B due to a uniform stray field), or showed significant differences between I_{c+} and I_{c-} of the order of 20–50% difference in the size of some corresponding fringes, several times the measurement precision. The large effect reflects the fact that flux is trapped in units of Φ_0 . We experienced good success in avoiding trapped flux by cooling the sample through the superconducting transition slowly in the low-field environment and by taking care to align the sample surfaces parallel to the applied field B .

Self-field effects¹² are distortions of $I_c(B)$ due to gradients of Φ induced by the magnetic fields of the

junction currents. The strength of these effects is characterized by λ_J , the Josephson penetration depth, given by $\lambda_J = [\mu_0 J(2\lambda + d)/\Phi_0]^{-1/2}$, where J is the local current density, assumed uniform for simplicity. If the junction dimensions are small compared to λ_J , the self-field distortion of the $I_c(B)$ is relatively small.¹³ In our crossed-strip geometry the current feed to the junction is asymmetric with respect to the applied B . Here the first-order effect of self-fields can be approximated by assuming that the junction current I produces a small uniform magnetic field B_I , of magnitude $B_I \approx \mu_0 I/b$, which aids or opposes the applied B . This produces a slight tilt of the $I_c(B)$ in the opposite sense for I_{c+} and I_{c-} , preserving the symmetry (7). The distortion is largest for the central maximum. Experimentally the extent of the effect is revealed by the an offset ΔB_I between the maxima of I_{c+} and I_{c-} . Corrections may be made by adjusting the value of B for a given I_c proportionally. Generally in our experiments this tilt was small.

Thermal or other voltage noise impressed on the junction causes fluctuations of Φ , reducing the observed I_c from the noise-free value.¹⁴ Since the phase-coupling energy $-I_c(B)\Phi_0/2\pi$ determining the stability of the supercurrent against these fluctuations depends on B , so does the factor by which I_c is reduced, being larger for smaller I_c . The reduction is hard to predict quantitatively, however, as it depends sensitively on such factors as the impedance and spectrum of the noise source, the capacitance and damping by quasiparticle resistance of the junction, and the measurement time-scale. Experimentally we find that a characteristic of junctions affected by noise is that values of $I_c(B)$ which lie below a certain current level tend to be strongly reduced, causing an obvious distortion of the shapes of the $I_c(B)$ minima, while above this range little reduction is apparent. In typical cases I_c is reduced to zero over an interval of B about a minimum. In these experiments the range of noise-limited currents was $I_c \lesssim 1-10 \mu\text{A}$, depending on the individual junction. To avoid such effects we tried to use junctions of relatively large I_c , consistent with avoiding self-field effects.

Besides tunneling, a second path for supercurrent flow is provided by any shorts through the barrier. The $I_c(B)$ of a shorted junction depends on the relative sizes of the tunneling and short critical supercurrents and the shape of the short-current phase relation. If the current phase relation is sinusoidal, then the high-current-density shorts behave as δ -function-like features of $\mathcal{J}(x)$. If the short-current phase relation is not sinusoidal, either intrinsically or as a result of self-field effects, $I_c(B)$ may be affected in various ways. From the related case of two small separated junctions with nonsinusoidal effective-current phase relations,¹⁵ one might ex-

pect features in $I_c(B)$ such as cusplike minima, asymmetric fringe shapes with respect to the direction of B , or displacement of the maximum value of I_c from $B=0$. If the short critical current is smaller than a few percent of the tunneling supercurrent, such effects might not be noticeable and probably the short would appear as a sharp feature in the constructed $\mathcal{J}(x)$.

The $I_c(B)$ which we use for the determination of $\mathcal{J}(x)$ are chosen to be free as far as possible of these effects. Specifically, we require that they obey (7), that their self-field tilt correspond to $\Delta B_I \lesssim 20\%$ of the oscillation period, and that they have no obvious major depression of the minima of I_c from noise effects.

IV. DATA

In Figs. 1, 4, and 7 we show plots of $I_c(B)$ for three different junctions. The data points are taken directly from the continuous recorder tracings and are the average of $I_{c+}(B)$ and $I_{c-}(B)$. In all three cases I_{c+} and I_{c-} have the same form (after corrections are made for a small self-field tilt) except in the immediate vicinity of the minima. Near these points a cross-talk effect in the converter induces a slight base line shift which is removed by the averaging. Also in these figures we show the positions of the maxima for a Fraunhofer form of corresponding $I_c(0)$ and magnetic field period.

In Fig. 1 we show $I_c(B)$ at 1.43°K, for one of our better Sn-oxide-Sn junctions. The junction dimensions were $a = 0.26 \pm 0.01$ mm and $b = 0.41 \pm 0.01$ mm and the film thicknesses ≈ 2000 Å. The oxide barrier was formed on the film of width a , i.e., the strip parallel to the applied B , by exposing the film to an oxygen plasma discharge before cross-evaporating the second strip. The $I_c(B)$ has approximately the ideal Fraunhofer form. The maximum critical current was 3.39 ± 0.01 mA, and the average magnetic field spacing between successive minima

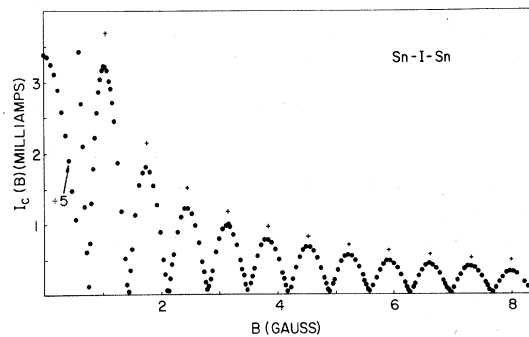


FIG. 1. $I_c(B)$ pattern at 1.43°K for a Sn-oxide-Sn junction for positive B . The central maximum is reduced by a factor of 5. Crosses indicate the positions and heights of the maxima of a Fraunhofer pattern.

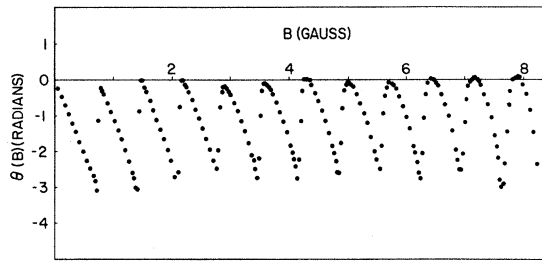


FIG. 2. Constructed phase $\theta(B)$ for the $I_c(B)$ pattern of Fig. 1.

was 0.695 ± 0.01 G corresponding to a value of $\approx 1140 \pm 50$ Å for $2\lambda + d$, reasonable for Sn. Corrections for a self-field tilt of $\Delta B_f = 0.08$ G have been applied.

Three deviations from the Fraunhofer form are notable in Fig. 1. First, the minima do not vanish exactly, showing that $\mathcal{J}(x)$ has an odd part. The values of I_c at the minima are of the order of $10 \mu\text{A}$, values on the upper edge of those I_c 's which are appreciably reduced by noise. Second, the secondary maxima are somewhat small, being $\sim 10\%$ low for the first and increasing to $\sim 30\%$ low for the tenth. Third, the spacing of the minima is not uniform, e.g., the first minimum occurs at 0.725 ± 0.01 G compared to the average spacing of 0.695 G.

A construction of $\mathcal{J}(x)$ was performed in the manner described in Sec. II, using the $I_c(B)$ to construct the phase $\theta(\beta)$ via (5). The phase construction was performed by digital computer using Simpson's-rule integration taking $I_c(B)$ at intervals of 0.03 G, or about 23 points per fringe, with the integration extending out to the 11th sidelobe in each direction. Figure 2 shows the constructed phase, and Fig. 3(a) shows the barrier profile $\mathcal{J}(x)$ resulting from this amplitude and phase. For convenience we plot both I_c and θ against B in gauss rather than in the normalized units β . This leads to an ambiguity in the scale of x in the transform which is of course removed by knowing the actual junction width.

The $\mathcal{J}(x)$ is the Fourier series

$$\sum_n I_c(\beta_n) \exp\{i[\theta(\beta_n) - \beta_n x]\},$$

where the β_n are the evenly spaced points at which $I_c(\beta)$ is sampled extending to the last point β_c . As always with Fourier series, the finite cutoff at β_c in effect convolutes the true $\mathcal{J}(x)$ with a $(\sin \beta_c x) / \beta_c x$ function, leading to a smoothing of sharp features and a Gibbs's phenomenon¹¹ at discontinuities such as the junction edges, this being an overshoot of the order of 7% on either side of a discontinuity. The resolution attained in $\mathcal{J}(x)$ is approximately equal to the barrier width divided by the number of fringes used in the series, in this case $\approx 0.04a$.

The shape of $\mathcal{J}(x)$ in Fig. 3(a) approximates a

uniform barrier, with deviations inside the junction edges on the order of 10%. The center of the junction appears to carry a larger current than the edges. Some structure is observed beyond the well-defined edges of the junction, due partly to the Gibbs's phenomenon and partly to errors in the construction. These are mostly less than 5% of the barrier height except the larger sharp negative feature on the left-hand side.

The error in the constructed $\mathcal{J}(x)$ compared to the real $\mathcal{J}(x)$ depends on the following considerations. It is inherent in the procedure used that the constructed $\mathcal{J}(x)$ will give precisely the input $I_c(B)$ pattern. Any errors other than those arising from a distorted $I_c(B)$ come from distortions in the phase such as must occur due to the finite cutoff in the $I_c(B)$ data used for construction of the phase. To understand the consequences of phase distortion, note that if $\mathcal{J}(x)$ were a purely even function about $x = \frac{1}{2}a$, the phase $\theta(\beta)$ would vary linearly with slope $-\frac{1}{2}a$ between minima, jumping discontinuously by π at each minimum. Since the constructed $\theta(\beta)$ has roughly this form the $\mathcal{J}(x)$ is indeed approximately even. Now the even and odd parts of $\mathcal{J}(x)$ about $x = \frac{1}{2}a$ are

$$\mathcal{J}_e(x) = \int_{-\infty}^{\infty} d\beta I_c(\beta) \cos[\theta(\beta) + \frac{1}{2}\beta a] \cos \beta x$$

and

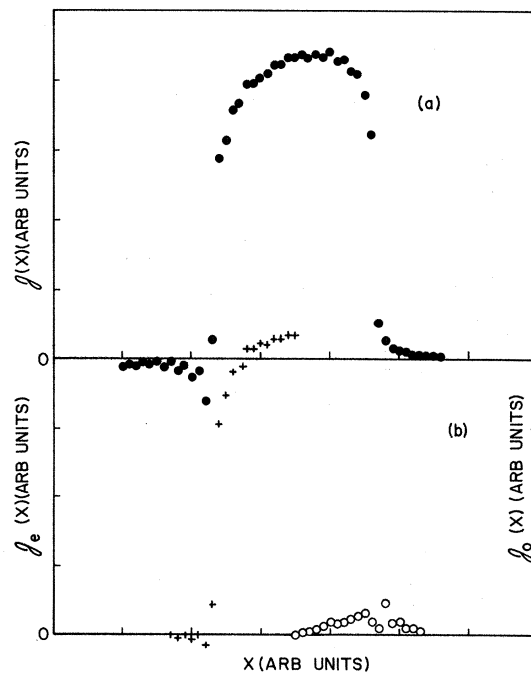


FIG. 3. (a) Current density profile $\mathcal{J}(x)$ deduced from the data of Figs. 1 and 2. (b) Decomposition of $\mathcal{J}(x)$ into even (crosses) and odd (circles) contributions.

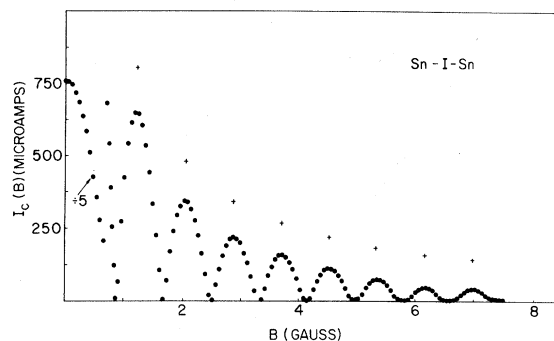


FIG. 4. $I_c(B)$ pattern at 1.46°K for a Sn-oxide-Sn junction for positive B . The central maximum is reduced by a factor of 5. Crosses indicate the positions and heights of the maxima for a Fraunhofer pattern.

$$\mathcal{J}_0(x) = \int_{-\infty}^{\infty} d\beta I_c(\beta) \sin[\theta(\beta) + \frac{1}{2}\beta a] \sin\beta(x).$$

Since $\theta(\beta)$ has approximately the form expected for an even function, $\theta(\beta) + \frac{1}{2}\beta a$ is approximately equal to some integral multiple of π . Then $\cos[\theta(\beta) + \frac{1}{2}\beta a]$ and hence $\mathcal{J}_e(x)$ are relatively insensitive to small deviations of $\theta(\beta)$ from linearity, while $\sin[\theta(\beta) + \frac{1}{2}\beta a]$ and $\mathcal{J}_o(x)$ will be more sensitive. The effect of a slight error in the form of $\theta(\beta)$ for these nearly even functions, then, will be to produce a spurious odd part with little effect on the even part. Consequently the even part of $\mathcal{J}(x)$ is more to be trusted than the odd part. This is especially true for sharp features in the odd part, since the phase reconstruction must necessarily be less accurate at higher values of β , closer to the cutoff of the $I_c(B)$.

In Fig. 3(b) we show a decomposition of $\mathcal{J}(x)$ into even and odd parts, where the center point is chosen to match the sharp increases at the two edges. The even part is a relatively smooth square barrier with somewhat rounded shoulders and little fine structure. The odd part contains somewhat more prominent fine structure although it has a much smaller overall amplitude. In particular, the sharp negative feature just beyond the junction edges is present largely in the odd part, suggesting that it is an artifact of the phase construction. The tendency of the supercurrent to be more concentrated in the junction center shown by Fig. 3 is reflected in the somewhat oversized value of B at the first minimum, some 4% larger than the average spacing of the minima.

Figure 4 shows the $I_c(B)$ for a second Sn-oxide-Sn junction at 1.46°K. The junction dimensions were $a = 0.22 \pm 0.01$ mm and $b = 0.41 \pm 0.01$ mm with a film thickness of ≈ 2000 Å. The oxide was grown in a plasma discharge on the strip lying parallel to the applied B . The $I_c(B)$ again has roughly the Fraunhofer form with some deviations. The maximum I_c was 0.758 ± 0.003 mA and the average mag-

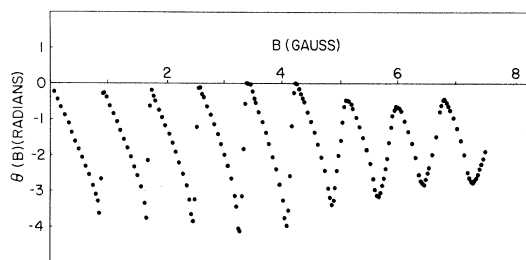


FIG. 5. Constructed phase $\theta(B)$ for the $I_c(B)$ pattern of Fig. 4.

netic field period was 0.83 ± 0.01 G corresponding to a $2\lambda + d$ of 1130 ± 50 Å. The self-field tilt was negligible, $\Delta B_I < 0.03$ G.

The amplitudes of the secondary maxima of $I_c(B)$ here again fall off faster than for the Fraunhofer form, the first being about 20% low and the others dropping off still more steeply. The minima are relatively deep, with the critical current actually being strictly zero for the higher-order minima. The flat-bottomed shape of the higher-order minima, in fact, is characteristic of noise decoupling. The smaller over-all critical current makes noise a more serious problem for this junction than the first. Since the phase-construction integral (5)

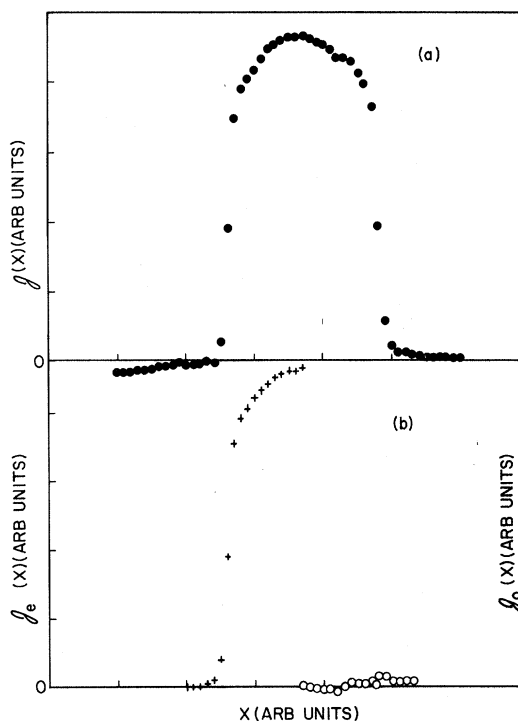


FIG. 6. (a) Current density profile $\mathcal{J}(x)$ deduced from the data of Figs. 4 and 5. (b) Decomposition of $\mathcal{J}(x)$ into even (crosses) and odd (circles) contributions.

cannot cope with zero I_c over a finite range, we have arbitrarily given a small value to I_c in these regions, as shown in Fig. 4. Consequently the constructed $\mathcal{J}(x)$ is more subject to uncertainty than for the junction of Figs. 1-3.

In Fig. 5 we show θ constructed from this $I_c(B)$, and in Fig. 6(a) and 6(b) the $\mathcal{J}(x)$ and its odd and even parts. The value of I_c at intervals of 0.03 G out to the tenth fringe were used in the construction, giving a resolution of some 23 points in the barrier. Here again we have a relatively smooth square barrier although it is somewhat more rounded than that of Fig. 3. The concentration of current near the junction center is supported by the larger spacing, by some $4\frac{1}{2}\%$, of the first minimum of $I_c(B)$ compared to the average spacing between minima.

For both these junctions having plasma-discharge grown oxides, the current is carried more strongly in the center of the barrier. This indicates a preferential oxidation of the edges of the film in the discharge. It is not surprising that there should be some spatial dependence of the oxide growth in view of the complex electric field patterns and plasma nonuniformity which undoubtedly exist around the film in the oxidation process.

We have performed similar measurements of Pb-oxide-Pb junctions having a thermally grown oxide. In these cases also we find a relatively uniform current density in the better junctions, often with a slight tendency for concentration of current away from the junction center. Somewhat more difficulty is encountered in these measurements because the higher transition temperature of Pb makes it more difficult to avoid trapped flux effects.

It should be noted here that the use of rectangular junctions has the disadvantage that for perfectly uniform barriers the $I_c(B)$ is expected to vanish periodically. This leads, as we have seen, to problems with thermal noise distortion. Additionally, the phase-construction integral (5) is sensitive to the

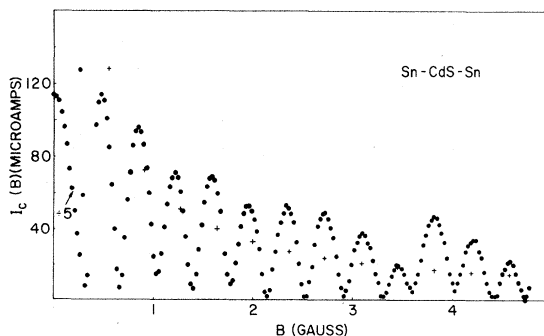


FIG. 7. $I_c(B)$ pattern for Sn-CdS-Sn junction. The central maximum is reduced by a factor of 5. Crosses indicate the positions and heights of the maxima of a Fraunhofer pattern.

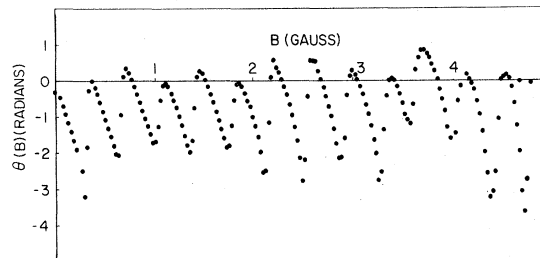


FIG. 8. Constructed phase $\theta(B)$ for the $I_c(B)$ pattern of Fig. 7.

small values of I_c , and its accuracy suffers if small errors are made in the measurement of the minima. Both problems would clearly be alleviated by the choice of an asymmetric shape of the junction, e.g., a triangle or a "T"-shaped junction for which $I_c(B)$ shows oscillations with relatively shallow minima. Such junction shapes are desirable if one wishes to measure $\mathcal{J}(x)$ with greater accuracy, but for our purposes we find the method is sufficiently accurate that we may confine the present discussion to the more familiar rectangular junction.

The $I_c(B)$ pattern of Fig. 7 arises from a Sn-Sn junction whose barrier is formed from insulating CdS in the manner reported by Giaever.¹⁰ The remarkable feature of this system is that the CdS is photosensitive. The exposure of the junction to light at low temperatures can decrease its resistance and enhance its supercurrent capacity by two or three orders of magnitude. The low-resistance state is metastable at liquid-He temperatures, the high-resistance state being recoverable by thermal cycling above $\sim 100^\circ\text{K}$. It has been suggested that the illumination in some fashion readjusts the Fermi level in the CdS, consequently altering the tunneling probability. In our junction the dimensions were $a = 0.54 \pm 0.01$ mm and $b = 0.42 \pm 0.01$ with a Sn thickness of $\approx 2000 \text{ \AA}$ for the bottom film and $\approx 500 \text{ \AA}$ for the top film. The smaller thickness of the top film was intended to provide transparency for the illumination of the 130-\AA -thick CdS. The $I_c(B)$ pattern here, taken at 1.45°K after the resistance had been reduced by illumination, also resembles the Fraunhofer form. The maximum critical current was 0.114 ± 0.002 mA and the average magnetic field period was 0.35 ± 0.01 G, corresponding to a value of $1090 \pm 60 \text{ \AA}$ for $2\lambda + d$. This small value presumably reflects the fact that the top film is not thick compared to λ .¹⁶

The secondary maxima of $I_c(B)$ beyond the first have amplitudes rather larger than those of the Fraunhofer pattern. The minima are deep but not zero at the lower values of B , and of irregular heights. Although the minima are in the $1\text{-}10 \mu\text{A}$ range their shapes do not appear to be obviously

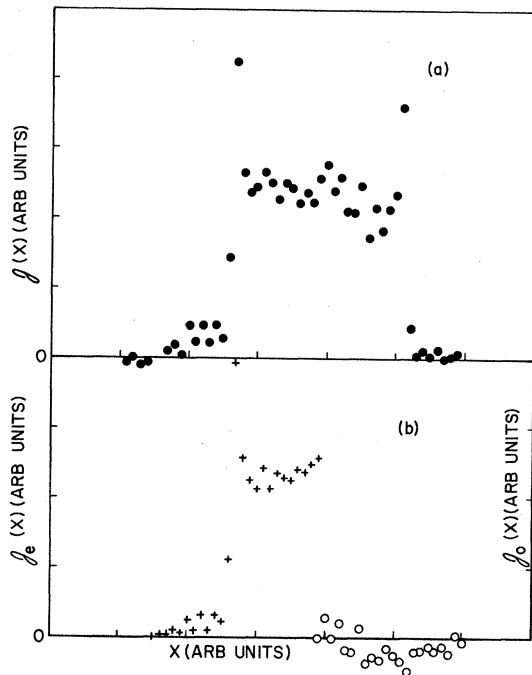


FIG. 9. (a) Current density profile $\mathcal{J}(x)$ deduced from the data of Figs. 7 and 8. (b) Decomposition of $\mathcal{J}(x)$ into even (crosses) and odd (circles) contributions.

distorted by noise. The difference between this junction and the Sn-oxide-Sn junctions in this respect is not fully understood but may have to do with the altered capacitance and the substantially smaller shunt resistance at low voltages present in this junction.

Figure 8 shows the phase $\theta(\beta)$ for the $I_c(B)$ of Fig. 7. The $\mathcal{J}(x)$ constructed from this amplitude and phase is shown in Fig. 9(a), and its odd and even parts $\mathcal{J}_o(x)$ and $\mathcal{J}_e(x)$ in Fig. 9(b). Here the points of I_c used in the construction were taken at 0.026 G intervals out to the 12th sidelobe, giving a resolution of 25 points in the barrier. The notable features are a sharp narrow rise in $\mathcal{J}(x)$ just at the two edges of the junction and considerable structure in the interior of the junction. Both features are present in $\mathcal{J}_e(x)$ as well. From the $I_c(B)$ we observe that the first minimum occurs at a B some 11% smaller than the average spacing, indicative of a concentration of current away from the junction center. Also, the excess heights of the secondary maxima require that there be fine structure within the junction. In Fig. 10 we show the $\mathcal{J}(x)$ derived by the alternate method discussed in Sec. II, that of assuming $\mathcal{J}(x)$ even. Here again the sharp concentration of current at the junction edges and the structure within the junction are visible in agreement with the Hilbert transform procedure. From the failure of the minima to vanish identically, we expect an odd part of \mathcal{J} as well. For example, the first minimum is

1.5 μ A, which would correspond to a purely linear odd part that would give an 8½% difference between the two edges of the junction. The larger current at the second minimum shows that the odd part is not particularly linear however.

That the current distribution shows a sharp increase at the junction edges is reasonable in view of the extra intensity of the illumination of the CdS which must occur at the junction edges. Indeed, it has been reported¹⁷ that the effectiveness of light in decreasing the junction resistance and enhancing the Josephson current is considerably weakened if the edges of the junction are masked during the illumination, an effect which would depend of course on the transparency of the Sn film. Here the actual contribution of the edges to the total supercurrent is of the order of 15%, indicating that the film is sufficiently transparent that most of the junction is sensitized as well. The structure within $\mathcal{J}(x)$ suggests that either the illumination is not uniform or the photosensitivity of the CdS is not uniform within the junction. In any case there is a considerable and rapid variation in the supercurrent density within the junction.

In summary it has been shown that for Josephson tunneling junctions the uniformity of the tunneling barrier can be determined quantitatively from the $I_c(B)$ pattern. It has also been shown that good quality junctions can be obtained in the case of plasma-grown oxides of Sn and thermally grown oxides of Pb, and that the usual assumption of constant current amplitude is nearly valid. This method of analysis has also been applied to the light-sensitive Sn-CdS-Sn junctions reported by Giaver. Here we find the supercurrent density is very spatially dependent, possibly as a result of variations in the exposure of the CdS to the incident illumination.

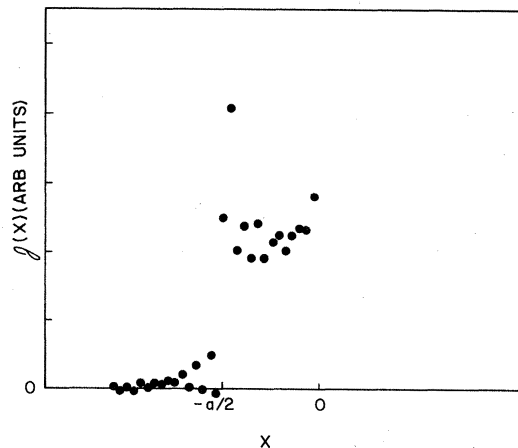


FIG. 10. $\mathcal{J}(x)$ derived from the data of Figs. 7 and 8 assuming the distribution is an even function. This current density profile is symmetric about $x=0$.

ACKNOWLEDGMENTS

We wish to thank J. M. Rowell, W. L. McMillan,

S. J. Allen, and H. D. Hagstrum for valuable discussions.

¹E. Burstein and S. Lundqvist, in *Tunneling Phenomena in Solids*, edited by E. Burstein and S. Lundqvist (Plenum, New York, 1969).

²I. Giaever and K. Megerle, *Phys. Rev.* **122**, 1101 (1961).

³P. H. Smith and J. L. Miles, *J. Electrochem. Soc.* **110**, 1240 (1963).

⁴R. B. Laibowitz and J. J. Cuomo, *J. Appl. Phys.* **41**, 2748 (1970).

⁵I. Giaever, in *Tunneling Phenomena in Solids*, edited by E. Burstein and S. Lundqvist (Plenum, New York, 1969).

⁶B. D. Josephson, *Phys. Letters* **1**, 251 (1962); B. D. Josephson, *Advan. Phys.* **14**, 419 (1965).

⁷P. W. Anderson, in *Progress in Low Temperature Physics*, Vol. 5, edited by C. J. Gorter (North-Holland, Amsterdam, 1967).

⁸P. W. Anderson and J. M. Rowell, *Phys. Rev. Letters* **10**, 230 (1963).

⁹J. M. Rowell, *Phys. Rev. Letters* **11**, 200 (1963).

¹⁰I. Giaever, *Phys. Rev. Letters* **20**, 1286 (1968).

¹¹A. Papoulis, *The Fourier Integral and Its Applica-*

tion (McGraw-Hill, New York, 1962).

¹²P. W. Anderson, in *Lectures on the Many-Body Problem*, edited by E. R. Caianello (Academic, New York, 1964); R. A. Ferrell and R. E. Prange, *Phys. Rev. Letters* **10**, 479 (1963).

¹³C. Owen and D. J. Scalapino, *Phys. Rev.* **164**, 538 (1967).

¹⁴V. Ambegaokar and B. I. Halperin, *Phys. Rev. Letters* **22**, 1364 (1969); J. Kurkijarvi and V. Ambegaokar, *Phys. Letters* **31A**, 314 (1970); Yu. M. Ivanchenko and L. A. Zil'berman, *Zh. Eksperim. i Teor. Fiz.* **55**, 2395 (1968) [*Sov. Phys. JETP* **28**, 1272 (1969)].

¹⁵T. A. Fulton, *Solid State Commun.* **8**, 1353 (1970).

¹⁶Here we consider the results of Owen and Scalapino [*J. Appl. Phys.* **41**, 2047 (1970)]. For a thin upper film of thickness L , $2\lambda + d$ becomes $\lambda + \lambda \tanh(L/2\lambda) + d$. From the previous oxide results we choose $\lambda \approx 570 \text{ \AA}$, yielding $\lambda + \lambda \tanh(L/2\lambda) + d = 935 \text{ \AA}$. In view of the probable unevenness of the thin film and the uncertainty of the thickness, this agreement is satisfactory.

¹⁷I. Giaever and H. R. Zeller, *J. Vac. Sci. Technol.* **6**, 502 (1969).

Low-Temperature Thermal Expansion and Longitudinal Magnetostriction of Palladium-Rhodium Alloys

E. Fawcett

Bell Telephone Laboratories, Murray Hill, New Jersey 07974

*and Department of Physics, University of Toronto, Toronto 5, Ontario, Canada**

(Received 17 June 1970)

The electronic thermal expansion and longitudinal magnetostriction of polycrystalline PdRh alloys are measured, and the volume dependence of the Coulomb-exchange interaction parameter is deduced.

The alloys PdRh are of considerable interest since the exchange enhancement of the magnetic susceptibility, which is already large in Pd, becomes even stronger as Rh is substituted for Pd. This increase in the susceptibility is associated with an increase in the density of states at the Fermi surface, which shows in the electronic specific heat. Both the susceptibility and the specific heat have a maximum at about the composition Pd_{0.95}Rh_{0.05}.¹

We describe in this paper measurements of the low-temperature thermal expansion and the longitudinal magnetostriction of polycrystalline samples of pure Pd² and the alloys Pd_{0.99}Rh_{0.01}, Pd_{0.97}Rh_{0.03}, and Pd_{0.95}Rh_{0.05}. We have previously assumed the magnetostriction to be isotropic in the cubic transition metals^{2,3} and obtained the volume dependence of the susceptibility by taking the volume magneto-

striction to be three times the longitudinal magnetostriction. However, Keller *et al.*⁴ have recently found that the magnetostriction of polycrystalline samples of Pd and the PdRh alloys is strongly anisotropic. Since their values for the longitudinal magnetostriction agree reasonably well with ours, we have employed their values for the volume magnetostriction to deduce the volume dependence of the susceptibility for comparison with the electronic Grüneisen parameter obtained from our thermal expansion data.

We measured the thermal expansion and the longitudinal magnetostriction (at 4.2°K in fields up to 35 kOe) using a capacitance dilatometer.³ The Grüneisen parameter γ is $3\alpha/\kappa C$, where α is the electronic thermal expansion coefficient (linear in temperature), κ the compressibility (assumed equal to that of Pd⁵), and C the electronic specific heat.¹